


ORIGINAL RESEARCH REPORT

Handling and performance characteristics of a new small caliber radiopaque embolic microsphere

Andrew L. Lewis  | Marcus Caine | Pedro Garcia | Koorosh Ashrafi |
Yiqing Tang | Lorcan Hinchcliffe | Wei Guo | Zainab Bascal | Hugh Kilpatrick |
Sean L. Willis

Biocompatibles UK Ltd., a BTG International Group Company, Camberley, Surrey, UK

Correspondence

Sean L. Willis, Biorr/ccompatibles UK Ltd., a BTG International Group Company, Lakeview, Riverside Way, Watchmoor Park, Camberley, Surrey GU15 3YL, UK.
Email: sean.willis@btgplc.com

Abstract

The in vitro and in vivo handling and performance characteristics of a small caliber radiopaque embolic microsphere, 40–90 μm DC Bead LUMI™ (LUMI40-90), were studied. Microsphere drug loading and elution and effects on size, suspension, and microcatheter delivery were evaluated using established in vitro methodologies. In vivo evaluations of vascular penetration (rabbit renal artery embolization), long-term biocompatibility and X-ray imaging properties, pharmacokinetics and local tissue effects of both doxorubicin (Dox) and irinotecan (Iri) loaded microspheres (swine hepatic artery embolization) were conducted. Compared to 70–150 μm DC Bead LUMI (LUMI70-150), LUMI40-90 averaged 70 μm versus 100 μm , which was unchanged upon drug loading. Handling, suspension, and microsphere delivery studies were successfully performed. Dox loading was faster (20 min) and Iri equivalent (<10 min) while drug elution rates were similar. Contrast suspension times were longer with no delivery complications. Vascular penetration was statistically greater (rabbit) with no unexpected adverse safety findings (swine). Microspheres \pm drug were visible under X-ray imaging (CT) at 90 days. Peak plasma drug levels and area under the curve were greater for LUMI40-90 compared to LUMI70-150 but comparable to 70–150 μm DC BeadM1™ (DC70-150). Local tissue effects showed extensive hepatic necrosis for Dox, whereas Iri displayed lower toxicity with more pronounced lobar fibrosis. LUMI40-90 remains suspended for longer and have greater vessel penetration compared to the other DC Bead LUMI sizes and are similarly highly biocompatible with long-term visibility under X-ray imaging. Drug loading is equivalent or faster with pharmacokinetics similar to DC70-150 for both Dox and Iri.

KEYWORDS

biocompatibility, DC Bead LUMI, drug loading and elution, microsphere penetration, pharmacokinetics, suspension and delivery, X-ray imageability

This is an open access article under the terms of the Creative Commons Attribution-NonCommercial-NoDerivs License, which permits use and distribution in any medium, provided the original work is properly cited, the use is non-commercial and no modifications or adaptations are made.

© 2020 The Authors. *Journal of Biomedical Materials Research Part B: Applied Biomaterials* published by Wiley Periodicals LLC.

1 | INTRODUCTION

Polymeric microspheres are widely used vehicles for the protection and tailored delivery of a vast array of drugs or biological molecules (Varde & Pack, 2004). The polymer matrix of the microsphere may be composed of synthetic materials such as polyesters or polyanhydrides, or natural polymers such as alginate or gelatin, which are often biodegradable in nature, releasing the drug as they resorb within the body (Prajapati, Jani, & Kapadia, 2015). The use of calibrated microspheres as devices for intra-arterial administration and controlled occlusion of blood vessels has been in clinical practice since the mid-1990's (Laurent et al., 1996). The microspherical devices may be composed of materials that are biodegradable or biostable in nature, depending on whether there is a desire to block the blood flow temporarily or permanently. In either case, the microspheres need to be suspended and diluted in a delivery medium and injected down narrow bore microcatheters without premature blockage; then into the blood stream where they are flow-directed into the target arteries and should block at a predictable level determined by their size and material properties (Beaujeux et al., 1996). For such applications, hydrogel microspheres are particularly suitable, as they suspend well and may possess some dimensional compressibility to facilitate microcatheter delivery. If the intention is to block arteries that feed a tumor, some microspheres may be loaded with chemotherapeutic agents to provide an additional benefit of sustained drug delivery at the target site (Fuchs et al., 2017).

Over the years, there has been a trend toward the use of smaller caliber microspheres in order to gain more distal distribution of the microspheres, particularly when the device is drug-eluting where good tumor coverage is essential. With this have been a few cautionary cases of fatal complications following the use of small microspheres, such as 40–120 μm Trisacryl-gelatin microspheres (Brown, 2004) and 40 μm polyphosphazene PMMA microspheres (Bonomo et al., 2010). Radiopaque drug-eluting embolic microspheres have been commercially available for a number of years (DC Bead LUMI) and are finding utility in clinical practice where location and extent of the embolic coverage are important considerations, as well as the potential to spot off-target embolization in real time (Aliberti et al., 2017; Iezzi et al., 2017; Levy et al., 2016a; Lewis et al., 2018). These microspheres are composed of a sulfonate-modified acrylamido-polyvinyl alcohol hydrogel (the basis of the Drug-eluting Embolization Microsphere product line DC Bead™) but in which triiodobenzyl groups have been coupled to the polymer backbone to confer radiodensity. The inherent radiopacity of the microspheres comes at a cost of increased density and stiffness (Ashrafi et al., 2017; Duran et al., 2016), making handling and administration more challenging as suspension times are shorter and potential for microcatheter blockage increased (Levy et al., 2016b). For this reason, the largest DC Bead LUMI currently offered in some territories is 100–300 μm in size range but since launch in 2015, the vast majority of clinical use has seen a transition to almost exclusive use of 70–150 μm DC Bead LUMI (LUMI70-150). Furthermore, DC Bead LUMI microspheres do not

undergo a reduction in size when loaded with drug unlike DC Bead [dose-dependent 25–30% decrease in diameter (Lewis et al., 2006)] and therefore are believed to perform more similarly to the larger sized equivalent DC Bead, that is LUMI70-150 performing similarly to DC100-300.

This has prompted the development of the smaller LUMI40-90 in order to better replicate the performance characteristics of DC70-150. The proposed benefits are that the smaller size helps to maintain a longer suspension, provide for ease of microcatheter delivery, and eliminate the tendency to clog the lumen, while benefiting from more distal vessel penetration. This study characterizes the performance of this product using various bench tests to evaluate handling and administration, together with both rabbit and swine arterial embolization models to understand its embolic and drug delivery behavior in vivo. This new 40–90 μm DC Bead LUMI size range has recently received approval in Canada.

2 | MATERIAL AND METHODS

2.1 | Materials

LUMI40-90, LUMI70-150, and DC70-150 were provided in 2 mL vials. Doxorubicin hydrochloride powder (>99% purity, Dox) was obtained from Hisun (China) and irinotecan hydrochloride (>99% purity, Iri) was obtained from ScinoPharm (Taiwan). Contrast agents used were Isovue™ 300, 370, and Iomeron™ 400 (Bracco Imaging, USA), Ultravist™ 370 (Bayer HealthCare Pharmaceuticals Inc., USA), Omnipaque™ 350 and Visipaque™ 320 and 370 (GE Healthcare, USA), Optiray™ 350 and Oxilan™ 350 (Guerbet LLC, USA). Microcatheters used for microsphere delivery were 2.0 and 2.4 Fr PROGREAT® Microcatheters (Terumo Corp., Japan).

2.2 | Microsphere size distribution analysis

LUMI40-90 and LUMI70-150 diameter size distributions were measured using an Olympus BX50 optical microscope and a 10 \times dry objective connected to a Colorview camera system as previously described with a minimum of 200 microspheres measured (Lewis et al., 2016).

2.3 | Evaluation of microsphere suspension using different contrast agents

LUMI40-90 and LUMI70-150 were suspended in various mixtures of different contrast agents using two 3 mL syringes connected with a 3-way stopcock. The syringe was then placed horizontally (to recreate clinical delivery conditions) and the time measured for 30% of the microsphere suspension to settle out.

2.4 | Microcatheter deliverability

Both LUMI40-90 and LUMI70-150 were delivered using different dilutions and contrast agent mixtures and the ease of delivery or cases of catheter blockage noted using a 3 mL syringe and Terumo Progreat microcatheters (2.4 and 2.0 Fr) set in a defined tortuous path in a water bath at 37°C. Force to deliver certain suspensions was obtained by attaching a force meter (Omega Engineering Inc.) to a custom mounted syringe adaptor to record the force required to expel the microsphere suspension. Furthermore, the Colorview camera system was set to focus on the transparent catheter hub and microsphere delivery was subsequently recorded as a record of the effect of dilution and bead size on catheter blocking.

2.5 | Comparative in vitro drug loading and drug elution properties

Drug solutions were prepared (25 mg/mL Dox or 10 mg/mL Iri) and microspheres loaded to 37.5 and 50 mg/mL, respectively, by removal of the packing solution and addition of the required drug loading solution. Residual drug levels remaining in the vial were measured over time using HPLC to obtain the relative rates and extents of drug loading. Drug elution was monitored by use of a recently described open-loop method (Ashrafi et al., 2017; Swaine et al., 2016) or the classic USP Type II "jar" method (Gonzalez et al., 2008) using phosphate-buffered saline at 37°C as eluent, which was pumped through an in-line UV/Visible spectrophotometry set at 453 nm for Dox or 365 nm for Iri. The absorption curves were converted to drug concentrations by use of standard curves to obtain comparative in vitro release profiles for each of the microsphere sizes.

2.6 | Biocompatibility studies

A biological evaluation was performed in accordance with International Standard ISO 10993-1 "Biological Evaluation of Medical Devices – Part 1: Evaluation and Testing Within a Risk Management Process" to determine the biocompatibility testing requirements for the LUMI family of microspheres used in these studies. The biological evaluation took into account the intended use as a permanent implanted device in contact with blood. Tests were performed to evaluate (a) genotoxicity, carcinogenicity, and reproductive toxicity, (b) interactions with blood, (c) in vitro cytotoxicity, (d) local effects following implantation in tissue for 2–26 weeks, (e) tests for irritation and skin sensitization, and (f) tests for systemic toxicity.

All biocompatibility testing studies were performed using microspheres, their packing solution or various extracts derived from the finished sterile medical device (non drug loaded) and in accordance with current Good Laboratory Practice (GLP) regulations (21 CFR Part 58) and were performed by NAMSA (Northwood, OH). The full experimental details of each test are detailed in the ISO 10993 guidance and are not reported here for brevity but are summarized in Table S1.

2.7 | Microsphere penetration in a rabbit renal artery model

A renal penetration model was used to determine the comparative extent of LUMI40-90 and LUMI70-150 microsphere penetration into the well-defined vascular tree within the kidney. This model has been well established in previous evaluations of embolic microsphere distribution in sheep (Laurent et al., 2006; Verret et al., 2011), swine (Maeda et al., 2013; Stampfl et al., 2009), and rabbits (Weng et al., 2013). As there is some overlap in the LUMI40-90 and LUMI70-150 size ranges (40–90 and 70–150 µm) arterial penetration was evaluated by renal artery embolization in New Zealand White rabbits where the smaller vessels were more suitable for detecting a separation between the two size ranges. The study was granted IRB approval in accordance to the local regulations for animal welfare (Protocol: #14-54 received positive notification without modification under decree number: 2013-118 dated February 1, 2013). Details of the model and study are described in detail elsewhere (Caine et al., 2018) but briefly, a total 50 µL of microspheres were delivered slowly using a 2.4 Fr microcatheter positioned 1 cm distally of the ostium to ensure a good distribution without premature embolization. Each product was administered into three individual kidneys. The animals were sacrificed 10 min postdelivery and the kidneys removed, fixed and sectioned and the distribution of microspheres across the various arterial levels determined by extensive pathological analyses. The levels were described as follows: Zone 1 - renal artery and its first branches; Zone 2 - interlobular arteries; Zone 3 - junction area at the border of the cortex and medulla; Zone 4 - deep cortex and proximal interlobular arteries; and Zone 5 - superficial cortex with distal interlobular arteries.

2.8 | Long-term biocompatibility and imaging in a swine hepatic arterial embolization model

A swine hepatic arterial embolization model was used to investigate the effect of LUMI40-90 tissue biocompatibility and long-term X-ray imaging visibility over a 90-day period, as previously reported for LUMI70-150 (Sharma et al., 2016). In brief, a 2.7 Fr microcatheter and a micro guidewire were used to select the lobar hepatic arteries supplying approximately 50% of the total liver volume. A 1:10 suspension of LUMI40-90 in Visipaque 320 was administered slowly (1 mL/min) under fluoroscopic guidance taking care to minimize reflux and avoid any extrahepatic nontarget embolization. All angiography and embolization procedures were performed using the GE OEC 9000 elite or GE OEC 9800 C-arm units with the standard GE cardiac software package allowing cine loops at 30 frames per second and the fraction of liver area embolized was estimated from the post-embolization angiography and DSA images by an experienced Interventional Radiologist. This was correlated and confirmed on the post-embolization CT images, which provided a good approximation of the total volume of liver embolized. These were performed using a GE Lightspeed 16 CT

scanner with helical acquisition and the images were reviewed in axial, coronal, and sagittal planes as well as in reconstructed maximum intensity projection images. CT scans with and without administration of IV contrast (nonionic IV contrast agent such as Omnipaque or Visipaque [GE Healthcare]) were obtained on the day of the procedure and at 30 and 90 days following embolization. Only the longest-term 90-day results are presented here. These were reviewed for LUMI40-90 visibility, location, area/volume of liver embolized, off-target embolization in adjacent organs, and other imaging findings, which may be related to hepatic embolization and associated ischemia.

Histopathology was conducted on tissues harvested at 30 and 90 days and necropsy performed with all major organs examined to check for any abnormalities. The liver and associated tissue and vessels were examined in specific detail for abnormalities and then fixed in neutral buffered formalin. Microscopic examination of fixed hematoxylin and eosin-stained paraffin sections was performed on sampled sections of tissues and the slides examined by a board-certified veterinary pathologist. Photomicrographs of representative lesions seen during the microscopic examination, including those considered to be treatment related, were taken.

2.9 | Pharmacokinetic evaluation and drug tissue effects in a swine hepatic arterial model

Pharmacokinetic (PK) analyses for both Dox and Iri delivered from LUMI40-90 were conducted as described in detail previously (Denys et al., 2017) using the swine hepatic artery embolization model described in the previous section. Plasma samples were taken at selected time points over a 24 hr period and analyzed for drug levels using HPLC-MS. The main PK parameters were reported compared to those previously obtained for both LUMI70-150 and DC70-150 under the same experimental conditions.

3 | RESULTS

3.1 | Comparison of microsphere size distributions and effect on drug loading and elution

Figure 1a shows the comparative microsphere size distributions for LUMI40-90 and LUMI70-150 as measured by optical microscopy (inset shows optical micrographs of each microsphere type). The mean

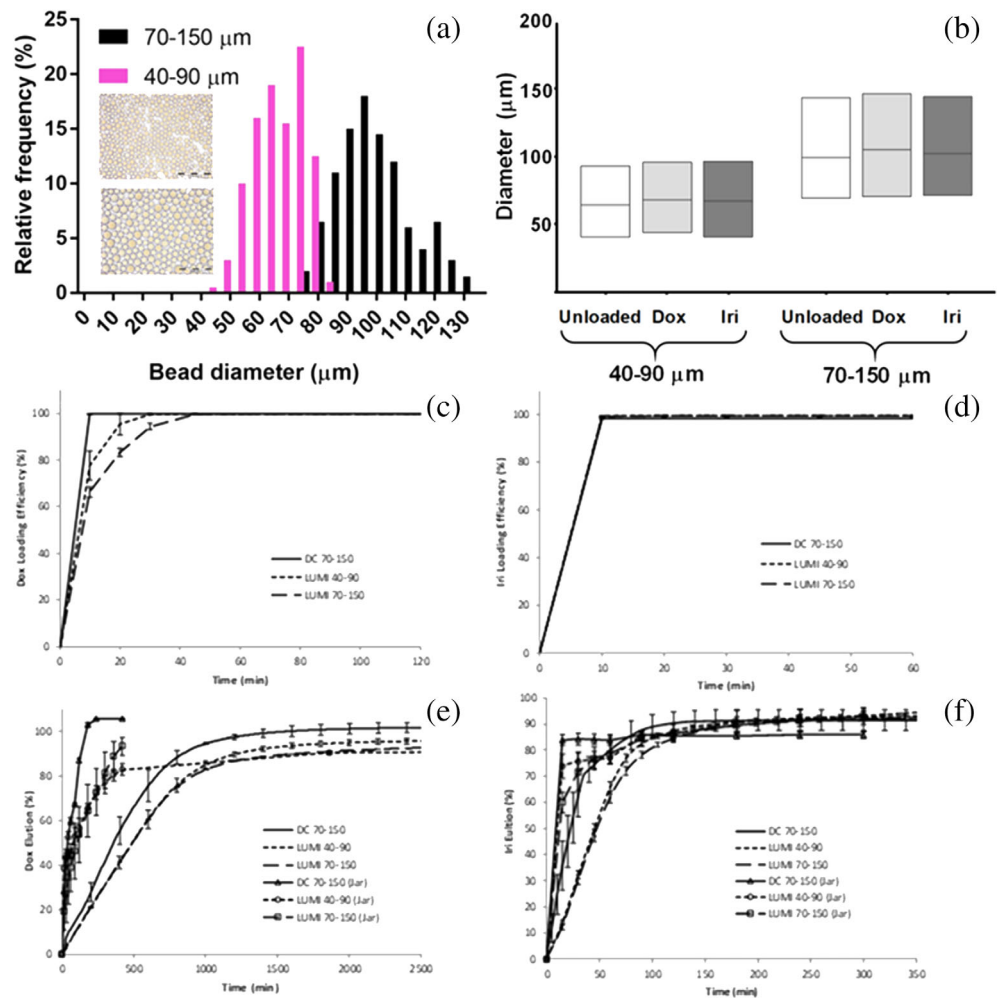


FIGURE 1 Comparison of LUMI40-90 and LUMI75-150: (a) Microsphere size distributions (inset, optical micrographs of each product, scale bar = 500 μm); (b) Effect of Dox (37.5 mg/mL) and Iri (50 mg/mL) loading on average microsphere size and range; (c) Dox (37.5 mg/mL) (d) and Iri (50 mg/mL) loading rates; (e) Dox and (f) Iri elution rates using “jar” and open-loop methods

size for LUMI40-90 was $68 \pm 9 \mu\text{m}$, compared to $98 \pm 13 \mu\text{m}$ for LUMI70-150 (Brown, 2004). Upon drug loading with either the recommended 37.5 mg/mL of Dox or 50 mg/mL of Iri, the average microsphere diameter and size range of either product was seen to be unaltered (Figure 1b). Figure 1c,d shows the drug loading times for each microsphere type. The DC Bead LUMI products took slightly longer to load Dox compared to DC Bead but Iri loaded within 10 min for each microsphere type. In each case, 100% of the drug was absorbed into the microspheres given sufficient time (max 1 hr for Dox). Figure 1e,f shows the comparative elution rates of both Dox and Iri for each microsphere size as determined by both open-loop and USP II ("jar") methods. In all cases, it was shown that 100% of the drug could be eluted from the microspheres (i.e., no irreversible drug-polymer interactions, data not shown).

3.2 | Microsphere suspension properties and microcatheter delivery

Table 1 shows the time in suspension in minutes for both LUMI40-90 and LUMI70-150, both unloaded and drug loaded and suspended in a variety of contrast agents. Visipaque was not used in the case of microspheres loaded with Iri as the high ionic concentration present in this contrast agent causes a rapid loss of drug from the microspheres (Kaiser, Thiesen, & Kramer, 2009).

Figure 2a shows the comparison of the force to deliver the LUMI40-90 versus LUMI70-150 microsphere suspensions in pure contrast agent (Omnipaque 350) and with various dilutions with saline, demonstrating no significant difference between microsphere sizes but with a gradual increase in force to deliver with an increasing amount of contrast agent in the suspension mixture. Figure 2b shows the effect of contrast agent: saline ratio on the mixture viscosity, showing how viscosity drops dramatically even with small amounts of saline addition to the contrast agent. A similar effect can be achieved by using lower strength contrast agents (e.g., Omnipaque 320 instead

of 350 is equivalent viscosity to a 20% dilution with saline). Despite these observations, there was no evidence of microsphere aggregation nor catheter obstruction during the test deliveries. Figure 2c shows optical micrographs of the hub section of a 2.7 Fr microcatheter, through which various suspension mixtures of Dox loaded LUMI40-90 and LUMI70-150 were delivered, providing a visual appreciation of the microsphere size and suspension concentration relative to the catheter hub. This clearly illustrates the reduced likelihood of premature catheter occlusion with increased microsphere dilution, however with LUMI40-90 even at a 1:40 dilution microspheres can be clearly seen filling the channel.

3.3 | Microsphere biocompatibility testing

Results of the series of Biocompatibility Tests according to ISO 10993 are summarized in Table S1. The LUMI microspheres passed all of the test criteria demonstrating the required degree of biocompatibility expected for permanent implants of this type.

3.4 | Comparative in vivo microsphere penetration potential

When evaluating the in vivo performance in a rabbit renal artery penetration model, LUMI40-90 is seen to embolize vessels of a smaller diameter than those embolized by LUMI70-150, with smaller microspheres occupying the smaller vessels of the more distal zones (zone 1: proximal-renal artery—zone 5: distal superficial cortex with distal interlobular arteries) (Figure 3a). When examining the percentage of microspheres found in each zone (Figure 3b), similar amounts were found for both microsphere sizes in zones 1, 2, and 3 as a result of "backfilling" that is, vessel IDs sufficiently large to accommodate multiple microspheres per cross-section leaving zones 4 and 5 as vessels of interest to be analyzed in isolation.

TABLE 1 Suspension times (min) for LUMI40-90 and LUMI75-150 in various contrast agents

Contrast agent	Chemical name	LUMI 40-90			LUMI 70-150		
		Unloaded	Doxorubicin	Irinotecan	Unloaded	Doxorubicin	Irinotecan
Isovue 300	Iopamidol	>2	>2	~2	>1	~1	~1
Isovue 370	Iopamidol	>5	>5	>4	>2	>2	>2
Ultravist 370	Iopromide	>7	>6	>6	>2	>2	>2
Visipaque 270	Iodixanol	>5	>5	-NA-	>2	>2	-NA-
Visipaque 320	Iodixanol	>10	>5	-NA-	>8	>5	-NA-
Optiray 350	Ioversol	>4	>4	>3	>1	>1	>1
Oxilan 350	Ioxilan	>5	>3	>3	>1	>1	>2
Omnipaque 350	Iohexol	>6	>7	>5	>3	>3	>2

Note: Deliverability of LUMI40-90 was successfully conducted in all tests in microcatheters down to 2.0-Fr (ID of $490 \mu\text{m}/0.019 \text{ in}$), the smallest evaluated in this study.

FIGURE 2 (a) Effect of microsphere size and suspension composition on force to deliver through a microcatheter; (b) Effect of contrast agent fraction in the suspension medium on viscosity; (c) Visual comparison of microsphere size suspensions and dilution on the mixture exiting the hub into the microcatheter lumen

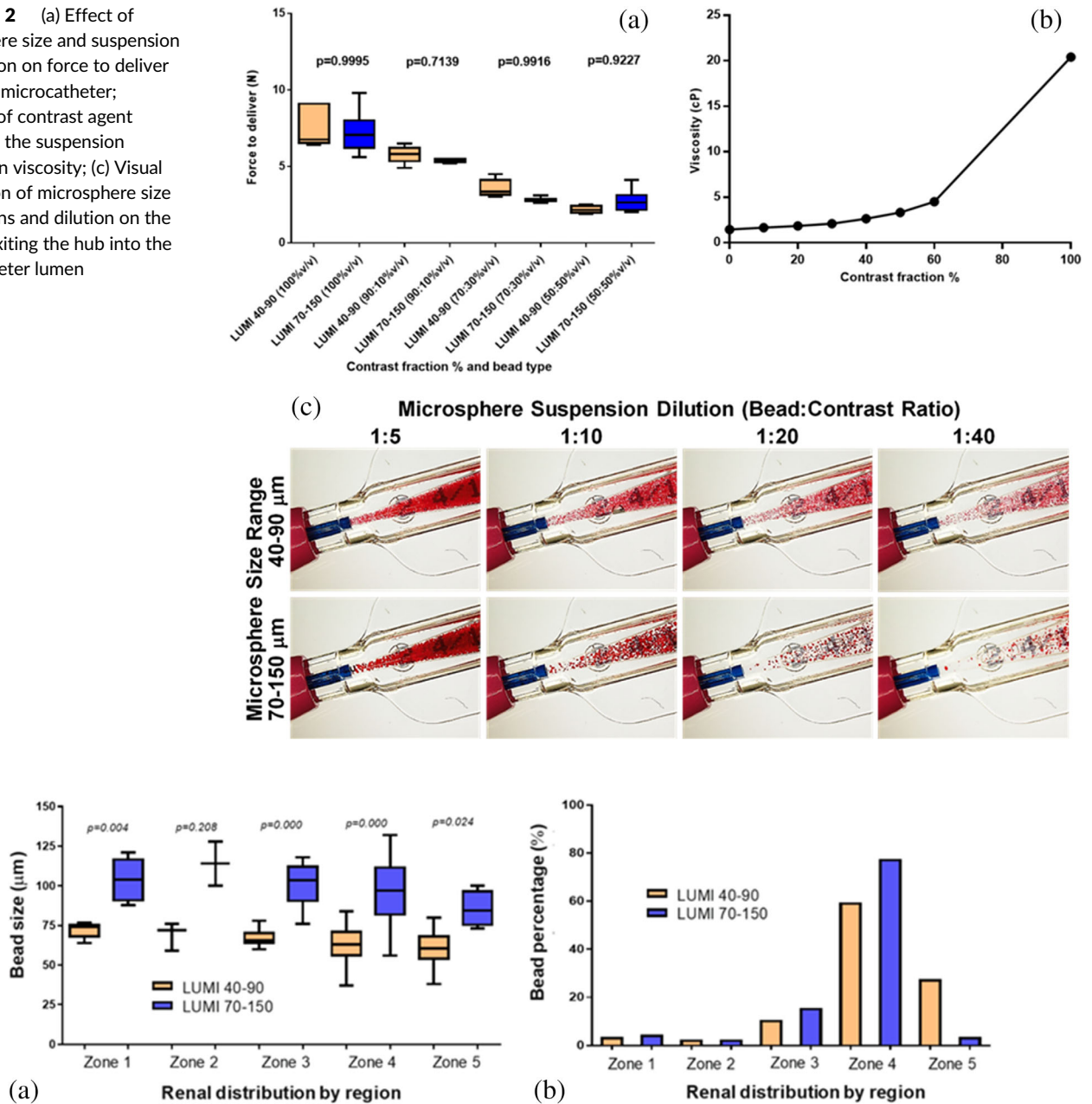


FIGURE 3 Comparative distributions by microsphere type in the renal model zones 1–5 (a) by microsphere size (b) by percentage of volume injected

3.5 | Long-term biocompatibility and CT-imaging evaluation

The product remained visible under CT with no diminished intensity of the X-ray visibility over the 90 day study period (Figure 4a–d). Detailed pathological examination at 30 and 90 days demonstrated a highly biocompatible material (as seen for the previous DC Bead LUMI sizes) with observations limited to the expected changes associated with occlusion of arterial vasculature in the liver and subsequent healing response, with no observed chronic inflammatory response, that is, a classic foreign body response with initial inflammation, fibrosis, and tissue remodeling (example histology shown in Figure 4e,f). The pathological examination

found no effects on any organs of the animal other than the embolization-induced changes within the targeted liver lobes.

3.6 | Comparison of key PK parameters and local effects of drug delivery to the liver

The swine hepatic arterial embolization model was also used to evaluate the PK properties of LUMI40-90 compared to LUMI70-150 utilizing DC70-150 as a control. The main PK parameters are summarized in Table 2 and the PK profiles for the various embolic microspheres loaded with Dox or Iri are shown in Figure 5.

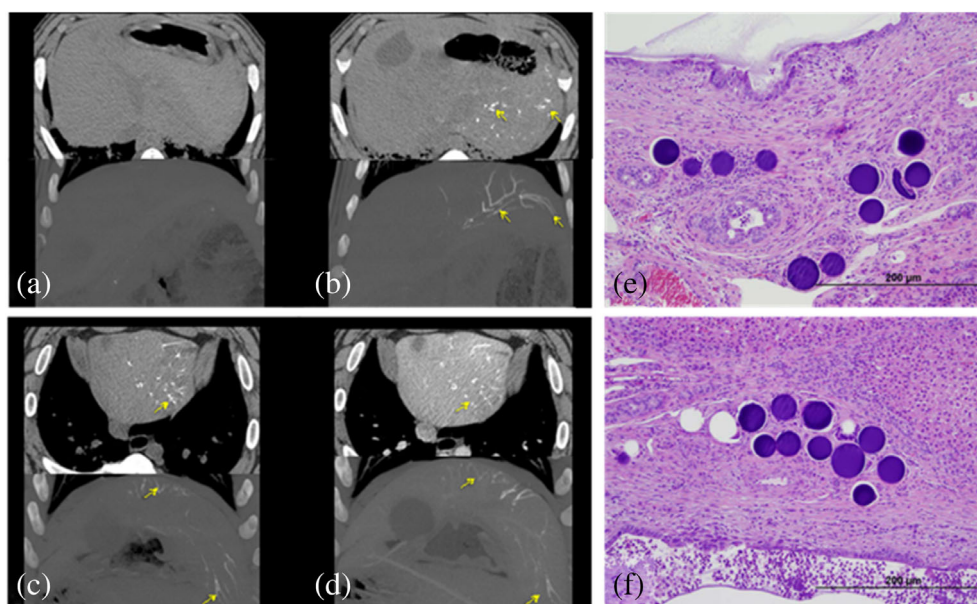


FIGURE 4 Multi Detector Computed Tomography (MDCT) (top) and maximum intensity projection (MIP) (bottom) imaging findings for LUMI40-90 (a) pre-embolization non-contrast CT images showing no abnormal observations in the liver. (b) Non-contrast CT images immediately post-embolization showing presence of LUMI40-90 in the main arteries of liver left lobe. (c) Non-contrast and (d) IV contrast-enhanced CT imaging 90 days post-embolization with LUMI40-90 still clearly visible, even in smaller more distal arteries. (e, f) typical histological sections containing LUMI40-90 microspheres (stained purple) embedded within tissue within the remodeled artery with the occasional instance of inflammatory cells contacting the microsphere surface

TABLE 2 Key pharmacokinetic parameters for DC70-150, LUMI70-150, and LUMI40-90 loaded with Dox or Iri

Microsphere type/size	Drug	Dose (mg)	C_{max} (ng/mL)	$C_{max}/dose$ ($ng^{-1} mL^{-1}/mg^{-1}$)	T_{max} (hr) ^a	AUC_{TLast} ($hr\ ng^{-1} mL^{-1}$)	$AUC_{TLast}/dose$ ($hr\ ng^{-1} mL^{-1}/mg^{-1}$)
DC70-150	Dox	57.7	99 (± 14.1)	1.72 (± 0.245)	0.083 (0.083–0.1)	135 (± 26.0)	2.35 (± 0.451)
LUMI70-150	Dox	37.5	74.6 (± 27.7)	1.99 (± 0.738)	0.067 (0.067–0.15)	186 (± 24.6)	4.93 (0.657)
LUMI40-90	Dox	37.5	140 (± 61.6)	3.73 (± 1.64)	0.08 (0.07–0.4)	165 (± 60.9)	4.40 (± 1.62)
DC70-150	Iri	91.1	1,310 (± 471)	14.3 (± 5.18)	0.100 (0.067–0.433)	5,970 ($\pm 3,790$)	65.5 (± 41.7)
LUMI70-150	Iri	50	474 (± 138)	9.47 (± 2.77)	1.067 (0.4–2.2)	2,860 (± 278)	57.3 (± 5.57)
LUMI40-90	Iri	50	1,290 (± 735)	25.7 (± 14.6)	0.18 (0.05–1.07)	5,470 ($\pm 1,630$)	109.0 (± 32.2)

Note: Mean (\pm SD) except a = Median (minimum–maximum).

The peak plasma concentration (C_{max}) and area under the curve (AUC) are somewhat similar for LUMI40-90 compared to DC70-150 (Dox: $C_{max} = 140 \pm 61.6$ vs. 99 ± 14.1 ; $AUC = 165 \pm 60.9$ vs. 135 ± 26.0 ; Iri: $C_{max} = 1,290 \pm 735$ vs. $1,310 \pm 471$; $AUC = 5,470 \pm 1,630$ vs. $5,970 \pm 3,790$). However, the plasma C_{max} and AUC for both drugs are somewhat higher for LUMI40-90 compared to LUMI70-150, although still very low compared to an IV administration of either drug.

Imaging of the animals treated with drug-loaded LUMI40-90 is shown in Figure 6, which clearly shows microspheres present throughout the liver lobe at both 1 hr and 14 days post-embolization with no effect of either drug on the imaging intensity (Figure 6a–d). Histological sections of treated areas of the liver at 14 days show

greater levels of tissue necrosis with Dox (Figure 6e) compared to Iri (Figure 6f), the latter tending to yield a more distinct pattern of interlobular fibrosis.

This swine PK study data indicated that at the standard Dox dose of 37.5 mg/mL or Iri dose of 50 mg/mL, the safety profile and histopathology was similar for both LUMI40-90 and LUMI70-150 with observations regarded as expected local tissue findings associated with an embolization procedure using a drug-loaded embolic microsphere. In addition, a comparison of treatment-related findings associated with administration of LUMI40-90 and DC70-150 groups at the standard Dox or Iri dose revealed no differences in the incidence or degree of the clinical pathology or histopathology changes for these two microsphere types.

FIGURE 5 Pharmacokinetic (PK) profiles for DC70-150, LUMI70-150, and LUMI40-90 loaded with (a) Dox and (b) Iri

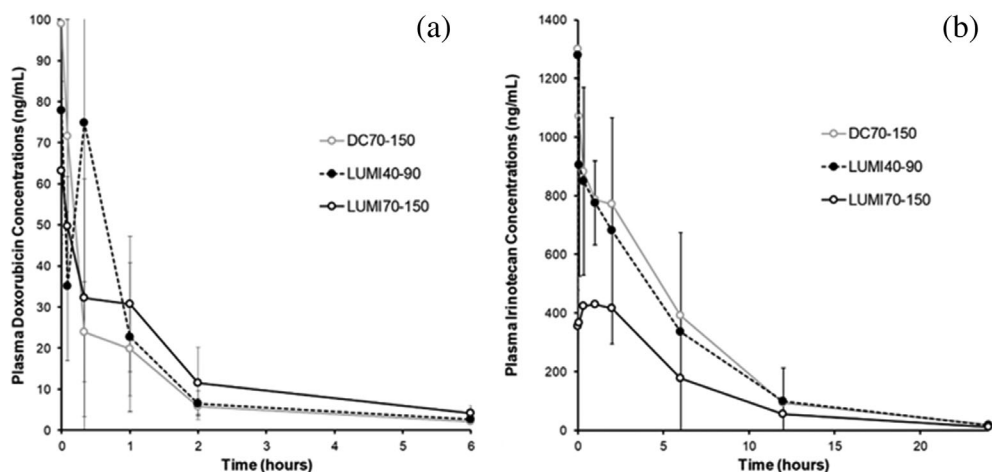
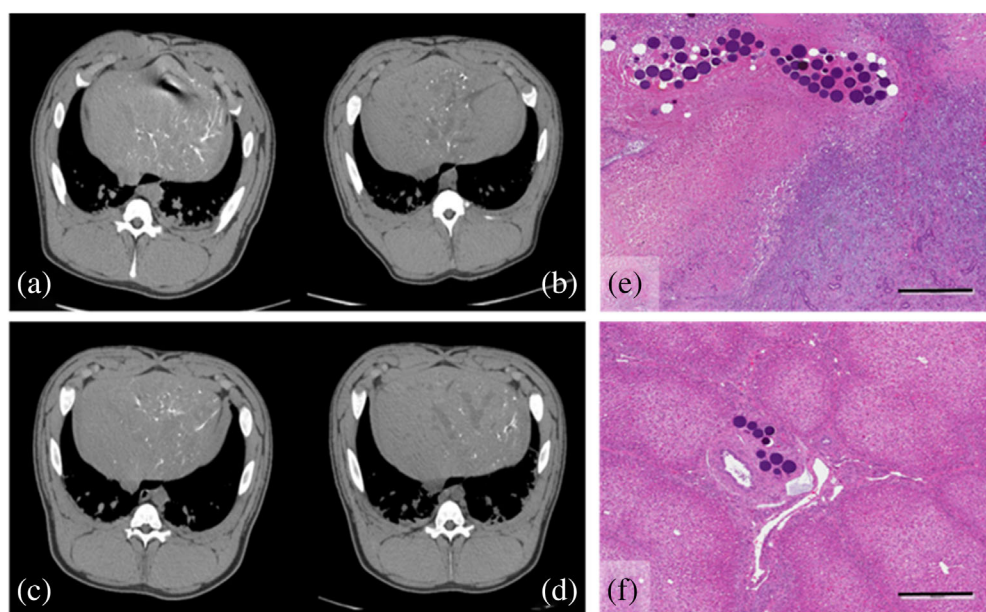


FIGURE 6 Non-contrast CT at (a) 1 hr post-embolization and (b) 14 days post-embolization with LUMI40-90 loaded with Dox (37.5 mg/mL). (c) 1 hr post-embolization and (d) 14 days post-embolization with LUMI40-90 loaded with Iri (50 mg/mL). (e) Histological section of a portion of the liver treated with LUMI40-90 + Dox showing widespread hepatic necrosis, bile duct hyperplasia, and interlobular fibrosis. (f) Histological section of a portion of the liver treated with LUMI40-90 + Iri showing comparatively less local tissue damage compared to Dox but with some interlobular fibrosis and bile duct hyperplasia



4 | DISCUSSION

LUMI40-90 is a new smaller diameter radiopaque microsphere that averages around 70 μm in diameter and is intended to provide more distal penetration combined with more detailed imaging of smaller vessels under X-ray based imaging techniques than the existing LUMI70-150. Both Dox and Iri loading is rapid (>98% loaded within 30 and 10 min, respectively) with the lower water content (~65%), higher density and increased hydrophobicity of the iodinated polymer matrix providing resistance to change in microsphere diameter upon drug loading. This is opposed to the high water content (~96%) DC Bead family of hydrogel beads, which shrink by ~25–30% upon drug loading as water is displaced from the polymer matrix when the drug binds to the sulfonate groups (Lewis, Gonzalez, et al., 2006). Drug elution as measured by *in vitro* methods suggests a slower elution than similar-sized DC Bead and that LUMI40-90 elutes at a similar rate to LUMI70-150 despite the smaller average size. This may be a consequence of the *in vitro* model used, which starts with a preformed

embolus of microspheres (Swaine et al., 2016); if a USP type II apparatus is used to rapidly elute drug into a large volume of eluent (Gonzalez et al., 2008) (emulating the initial flow of microspheres into the blood vessel and to the target site), there is a more rapid release of both Dox and Iri from the smaller LUMI40-90 due to increased surface area to volume ratio. These findings, therefore, confirm the observations made on the *in vivo* PK analysis for both Dox and Iri when delivered from LUMI40-90. The immediate burst of the drug from the microspheres as measured by the plasma C_{max} and the first few hours of release represented by the AUC are seen to increase for both drugs when eluted from LUMI40-90, relative to LUMI70-150. Note, however, the increase in these parameters is similar to the values seen for DC70-150 and therefore still very low in terms of overall systemic exposure when compared to the drug administered intra-arterially or by conventional transarterial chemoembolization (Hong et al., 2006; Johnson et al., 1991; Varela et al., 2007). The rationale for the use of a Drug-eluting Embolization Microsphere over systemic drug administration is to reduce both the peak plasma

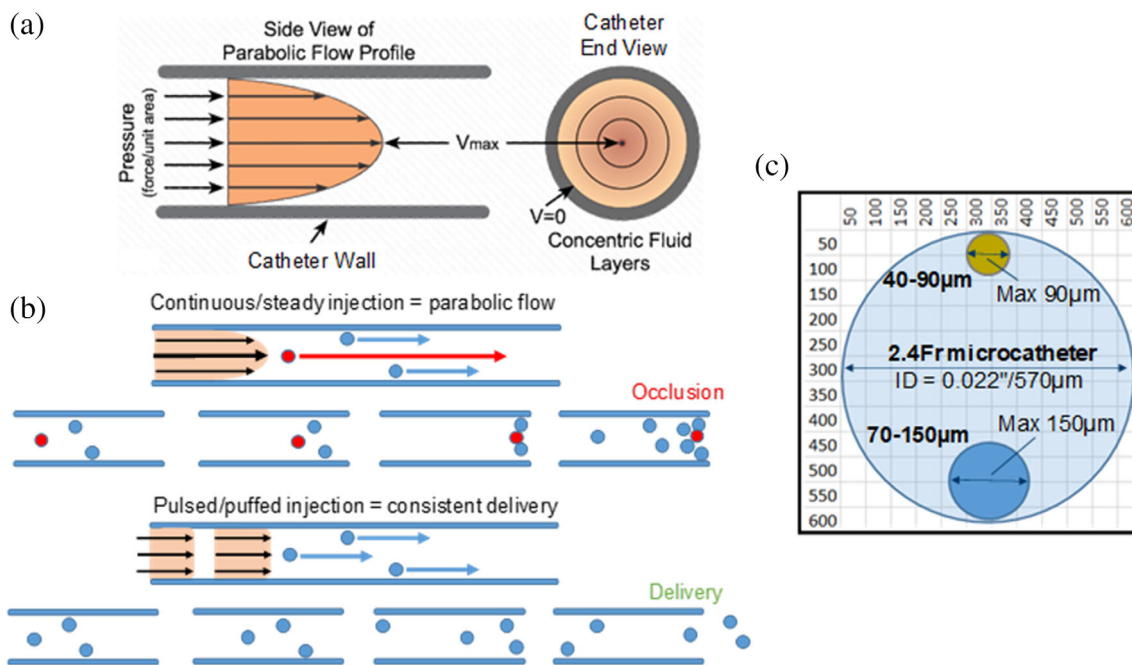


FIGURE 7 (a) Parabolic flow profile of laminar flow within a microcatheter showing velocity profiles across the cross section; (b) diagram illustrating the effect of steady versus pulsed injection relative speed of microsphere travel along the catheter; (c) relative confinement ratio of LUMI40-90 and LUMI70-150 as a function of a 2.4 Fr microcatheter internal lumen demonstrating ability of significantly smaller microspheres to avoid transient microcatheter occlusions compared to LUMI100-300

concentration (C_{\max}) and the prolonged drug exposure to the nontarget tissues (AUC), maximizing the drug delivery in the local vicinity of the tumor, assuming the malignancy is discreet in nature and has not metastasized around the body. Elimination of most of the drug from the circulation within 24 hr as seen here is, therefore, a desirable outcome and a hallmark for Drug-eluting Embolic Microsphere-based treatment versus conventional systemic administration.

While microsphere suspension in pure contrast agent provides the most stable suspensions and is recommended by the manufacturer in their Instructions for Use (IFU), it is clear that the high viscosity of this medium significantly increases the force required to inject the microspheres from the syringe with no difference between LUMI40-90 and LUMI70-150 (no size effect with these small caliber microspheres). Dilution with a small amount of saline (10%) or use of lower iodine content contrast agents (which are de-facto less viscous) significantly decreases the viscosity of the microsphere suspension while maintaining an acceptable suspension time. Indeed, Aliberti et al. have proposed that dilution with saline aided injection ease, enhanced mixing of the microspheres in the injection solution with blood and resulted in more volume of microspheres administered per treated tumor prior to reaching procedural endpoint for LUMI70-150 (Aliberti et al., 2017).

The IFU also recommends a minimum microsphere to contrast ratio dilution of 1:10 to ensure sufficient inter-microsphere spacing and prevention premature clogging of microspheres at the hub and within the narrow microcatheter lumen. Appropriate dilution can ensure sufficient spacing between microspheres so that they do not accumulate as they enter the catheter lumen, and the use of intermittent injection "puffs" generates a pulsatile non-laminar flow in the microcatheter lumen, which

consequently reduces the risk of catheter occlusion. Conversely, constant injection pressure will induce laminar flow within the microcatheter causing microspheres travelling in the center of the lumen to move faster than those near the walls, compromising the dilution (or separation effect) and causing microspheres to come together and bridge or arc within the lumen to initiate a blockage cascade (Figure 7a,b). This effect can be described by the Durand relation in Equation (1), for a particle dependent critical flow velocity (Miedema, 2013):

$$V_c = F_L \sqrt{2gD(s-1)} \quad (1)$$

where F_L is the Durand fitting factor affected by the particle size and concentration, D is the flow channel diameter, g is the acceleration due to gravity, and s is the density ratio of particle to fluid.

Pulsatility has become increasingly utilized during delivery of suspended microspheres and has been shown in several studies to reduce the accumulation of particles under flow (Corbett, Ajdari, Coskun, & Nayeb-Hashemi, 2010; Fujimoto, Kubo, Hama, & Takuda, 2010). This is particularly important when delivering stiffer particles with lower compliance to the microcatheter lumen during delivery, such as with DC Bead LUMI where the risk of permanent blockades could increase relative to the more compressible DC Bead, due to the radiopaque iodine component inherent within the DC Bead LUMI structure that increases hydrophobicity and decreases the overall water content of the hydrogel (Figure 7). Successful delivery of both microsphere sizes has been demonstrated in this study using a range of microcatheters with ID as low as 2.0 Fr catheter (clearly from Figure 7c both microsphere sizes are much smaller than the internal

diameter of the commonly used 2.4 Fr catheter, whereas the maximum size of the LUMI100-300 size would be greater than half of the lumen diameter). A previous study has reported the successful delivery of LUMI40-90 using an even smaller 1.9 Fr Prowler Select LP ES microcatheters (Codman, Raynham, MA) with ID at 419 μm /0.016 in using 1 mL delivery syringe (Brown, 2004). Although it is still recommended to follow the manufacturer's guidance for "puff-like" administration at 1 mL/min for the avoidance of potential catheter blockage and according to the theory of critical particle velocity under flow [Equation (1) and Figure 7].

The in vivo evaluation of the penetration potential of LUMI40-90 clearly demonstrated that these microspheres occupy smaller vessels than those of LUMI70-150 and hence penetrate deeper into the vascular tree as seen by the greater percentage of microspheres found in the most distal zone 5 of the kidney. It can be concluded that LUMI70-150 populates zones 4 and 5 in a 94:6 ratio whereas LUMI40-90 populates in a 67:33 ratio demonstrating a more distal penetration for the smaller size range, as expected.

This increase in distal penetration, however, is not associated with any new safety-related events as demonstrated by the 90-day hepatic embolization study in the swine model, with no differences in the observations of tissue effects compared to LUMI70-150. It should be noted, however, that one limitation of this large animal model is that it does not possess a tumor and hence lacks any shunting that is often observed in larger hepatocellular carcinoma masses. Careful observation for the presence of shunting is therefore recommended when using small caliber microspheres such as LUMI40-90, LUMI70-150, and DC70-150 (as per the manufacturer's IFU).

Drug loading into LUMI40-90 was seen to have no effect on the level of radiopacity and hence X-ray visibility (as also seen for the other DC Bead LUMI sizes) (Ashrafi et al., 2017). Visibility persists unaffected for at least 90 days as demonstrated in this study, and likely way beyond this time, as the product is a permanent radiopaque embolic that does not degrade in the body over time. The same swine hepatic arterial embolization model was used to evaluate LUMI40-90 as with a recent study on LUMI70-150 (Sharma et al., 2016), with very similar findings to that of LUMI70-150. Histopathological analysis of the liver tissue treated with unloaded LUMI40-90 over the 90 day period shows all the expected tissue responses due to embolization with embolic microspheres but with eventual complete encapsulation within the tissue and no signs of any chronic inflammatory response for the very biocompatible material from which DC Bead LUMI is composed. These observations are supported by the results of the extensive biocompatibility testing that was undertaken for the microspheres and summarized in Table S1. When LUMI40-90 is loaded with Dox, extensive hepatic necrosis is noted for treated areas of the liver as previously reported for DC Bead (Lewis et al., 2006). Local delivery of this highly cytotoxic drug kills hepatocytes and creates widespread necrosis and bile duct hyperplasia in the areas targeted by the microspheres. For LUMI40-90 loaded with Iri, again, the observations are consistent with those seen for DC Bead loaded with Iri (Taylor, Tang, Gonzalez, Stratford, & Lewis, 2007), with less toxicity compared to Dox but more distinct interlobular fibrosis occurring along with

instances of bile duct dilation that has been observed associated with accumulations of microspheres in the CT imaging.

5 | CONCLUSION

LUMI40-90 is a new small size caliber radiopaque microsphere of the DC Bead LUMI family for use in embolization procedures. Its smaller size allows for more distal penetration within the vessels while maintaining visibility for imaging intra-procedurally under fluoroscopy and with cone beam CT and long-term post-procedure imaging using MDCT. The smaller size is not associated with any additional safety concerns beyond those that are currently considered when using LUMI70-150 and maintains a favorable PK profile in these preclinical models for local delivery of either Dox when treating HCC or Iri if treating metastatic colorectal cancer to the liver.

CONFLICT OF INTEREST

All of the authors named on this manuscript are employees of Biocompatibles UK Ltd., the manufacturer of the test device that was the subject of this study. Some of these data were generated for use in filings with Regulatory agencies to demonstrate the safety of the device.

ORCID

Andrew L. Lewis  <https://orcid.org/0000-0001-5779-5631>

REFERENCES

- Aliberti, C., Carandina, R., Sarti, D., Pizzirani, E., Ramondo, G., Cillo, U., ... Fiorentini, G. (2017). Transarterial chemoembolization with DC bead LUMI radiopaque beads for primary liver cancer treatment: Preliminary experience. *Future Oncology*, 13(25), 2243–2252.
- Ashrafi, K., Tang, Y., Britton, H., Domenge, O., Bliino, D., Bushby, A. J., ... Lewis, A. L. (2017). Characterization of a novel intrinsically radiopaque drug-eluting bead for image-guided therapy: DC bead LUMI. *Journal of Controlled Release*, 250, 36–47.
- Beaujeux, R., Laurent, A., Wassef, M., Casasco, A., Gobin, Y. P., Aymard, A., ... Merland, J. J. (1996). Trisacryl gelatin microspheres for therapeutic embolization, II: Preliminary clinical evaluation in tumors and arteriovenous malformations. *American Journal of Neuroradiology*, 17(3), 541–548.
- Bonomo, G., Pedicini, V., Monfardini, L., Della Vigna, P., Poretti, D., Orgera, G., & Orsi, F. (2010). Bland embolization in patients with unresectable hepatocellular carcinoma using precise, tightly size-calibrated, anti-inflammatory microparticles: First clinical experience and one-year follow-up. *Cardiovascular and Interventional Radiology*, 33(3), 552–559.
- Brown, K. T. (2004). Fatal pulmonary complications after arterial embolization with 40-120- micro m tris-acryl gelatin microspheres. *Journal of Vascular and Interventional Radiology*, 15(2 Pt 1), 197–200.
- Caine, M., Zhang, X., Hill, M., Guo, W., Ashrafi, K., Bascal, Z., ... Lewis, A. L. (2018). Comparison of microsphere penetration with LC bead LUMI versus other commercial microspheres. *Journal of the Mechanical Behavior of Biomedical Materials*, 78, 46–55.
- Corbett, S. C., Ajdari, A., Coskun, A. U., & Nayeb-Hashemi, H. (2010). Effect of pulsatile blood flow on thrombosis potential with a step wall transition. *ASAIO Journal*, 56(4), 290–295.

- Denys, A., Czuczman, P., Grey, D., Bascal, Z., Whomsley, R., Kilpatrick, H., & Lewis, A. L. (2017). Vandetanib-eluting radiopaque beads: in vivo pharmacokinetics, safety and toxicity evaluation following swine liver embolization. *Theranostics*, 7(8), 2164–2176.
- Duran, R., Sharma, K., Dreher, M. R., Ashrafi, K., Mirpour, S., Lin, M. D., ... Geschwind, J. F. H. (2016). A novel inherently radiopaque bead for transarterial embolization to treat liver cancer - A pre-clinical study. *Theranostics*, 6(1), 28–39.
- Fuchs, K., Duran, R., Denys, A., Bize, P. E., Borchard, G., & Jordan, O. (2017). Drug-eluting embolic microspheres for local drug delivery - State of the art. *Journal of Controlled Release*, 262, 127–138.
- Fujimoto, H., Kubo, M., Hama, T., & Takuda, H. (2010). Transport phenomena of solid particles in pulsatile pipe flow. *Advances in Mechanical Engineering*, 2, 121326.
- Gonzalez, M. V., Tang, Y., Phillips, G. J., Lloyd, A. W., Hall, B., Stratford, P. W., & Lewis, A. L. (2008). Doxorubicin eluting beads-2: Methods for evaluating drug elution and in-vitro:In-vivo correlation. *Journal of Materials Science. Materials in Medicine*, 19(2), 767–775.
- Hong, K., Khwaja, A., Liapi, E., Torbenson, M. S., Georgiades, C. S., & Geschwind, J. F. (2006). New intra-arterial drug delivery system for the treatment of liver cancer: Preclinical assessment in a rabbit model of liver cancer. *Clinical Cancer Research*, 12(8), 2563–2567.
- Iezzi, R., Pompili, M., Annicchiarico, E. B., Garcovich, M., Siciliano, M., Gasbarrini, A., & Manfredi, R. (2017). 'Hug sign': A new radiological sign of intraprocedural success after combined treatment for hepatocellular carcinoma. *Hepatology Oncology*, 4(3), 69–73.
- Johnson, P. J., Kalayci, C., Dobbs, N., Raby, N., Metivier, E. M., Summers, L., ... Williams, R. (1991). Pharmacokinetics and toxicity of intraarterial adriamycin for hepatocellular carcinoma: Effect of coadministration of lipiodol. *Journal of Hepatology*, 13(1), 120–127.
- Kaiser, J., Thiesen, J., & Kramer, I. (2009). Stability of irinotecan-loaded drug eluting beads (DC bead) used for transarterial chemoembolization. *Journal of Oncology Pharmacy Practice*, 16(1), 53–61.
- Laurent, A., Beaujeux, R., Wassef, M., Rüfenacht, D., Boschetti, E., & Merland, J. J. (1996). Trisacryl gelatin microspheres for therapeutic embolization, I: Development and in vitro evaluation. *American Journal of Neuroradiology*, 17(3), 533–540.
- Laurent, A., Wassef, M., Saint Maurice, J. P., Namur, J., Pelage, J. P., Seron, A., ... Merland, J. J. (2006). Arterial distribution of calibrated tris-acryl gelatin and polyvinyl alcohol microspheres in a sheep kidney model. *Investigative Radiology*, 41(1), 8–14.
- Levy, E. B., Krishnasamy, V. P., Lewis, A. L., Willis, S., Macfarlane, C., Anderson, V., ... Wood, B. J. (2016a). First human experience with directly image-able iodinated embolization microbeads. *Cardiovascular and Interventional Radiology*, 39(8), 1177–1186.
- Lewis, A. L., Dreher, M. R., O'Byrne, V., Grey, D., Caine, M., Dunn, A., ... Wood, B. J. (2016). DC BeadM1™: Towards an optimal transcatheter hepatic tumour therapy. *Journal of Materials Science: Materials in Medicine*, 27(1), 1–12.
- Lewis, A. L., Gonzalez, M. V., Lloyd, A. W., Hall, B., Tang, Y., Willis, S. L., ... Stratford, P. W. (2006). DC bead: in vitro characterization of a drug-delivery device for transarterial chemoembolization. *Journal of Vascular and Interventional Radiology*, 17(2 Pt 1), 335–342.
- Lewis, A. L., Taylor, R. R., Hall, B., Gonzalez, M. V., Willis, S. L., & Stratford, P. W. (2006). Pharmacokinetic and safety study of doxorubicin-eluting beads in a porcine model of hepatic arterial embolization. *Journal of Vascular and Interventional Radiology*, 17(8), 1335–1343.
- Lewis, A. L., Willis, S. L., Dreher, M. R., Tang, Y., Ashrafi, K., Wood, B. J., ... Mikhail, A. S. (2018). Bench-to-clinic development of imageable drug-eluting embolization beads: Finding the balance. *Future Oncology*, 14, 2741–2760.
- Maeda, N., Verret, V., Moine, L., Bédouet, L., Louguet, S., Servais, E., ... Laurent, A. (2013). Targeting and recanalization after embolization with calibrated resorbable microspheres versus hand-cut gelatin sponge particles in a porcine kidney model. *Journal of Vascular and Interventional Radiology*, 24(9), 1391–1398.
- Miedema, S. A. (2013). An overview of theories describing head losses in slurry transport. A tribute to some of the early researchers. in OMAE 2013, 32nd International Conference on Ocean, Offshore and Arctic Engineering.
- Prajapati, V. D., Jani, G. K., & Kapadia, J. R. (2015). Current knowledge on biodegradable microspheres in drug delivery. *Expert Opinion on Drug Delivery*, 12(8), 1283–1299.
- Sharma, K. V., Bascal, Z., Kilpatrick, H., Ashrafi, K., Willis, S. L., Dreher, M. R., & Lewis, A. L. (2016). Long-term biocompatibility, imaging appearance and tissue effects associated with delivery of a novel radiopaque embolization bead for image-guided therapy. *Biomaterials*, 103, 293–304.
- Stampfl, S., Bellemann, N., Stampfl, U., Sommer, C. M., Thierjung, H., Lopez-Benitez, R., ... Richter, G. M. (2009). Arterial distribution characteristics of Embozene particles and comparison with other spherical embolic agents in the porcine acute embolization model. *Journal of Vascular and Interventional Radiology*, 20(12), 1597–1607.
- Swaine, T., Tang, Y., Garcia, P., John, J., Waters, L. J., & Lewis, A. L. (2016). Evaluation of ion exchange processes in drug-eluting embolization beads by use of an improved flow-through elution method. *European Journal of Pharmaceutical Sciences*, 93, 351–359.
- Taylor, R. R., Tang, Y., Gonzalez, M. V., Stratford, P. W., & Lewis, A. L. (2007). Irinotecan drug eluting beads for use in chemoembolization: in vitro and in vivo evaluation of drug release properties. *European Journal of Pharmaceutical Sciences*, 30(1), 7–14.
- Varde, N. K., & Pack, D. W. (2004). Microspheres for controlled release drug delivery. *Expert Opinion on Biological Therapy*, 4(1), 35–51.
- Varela, M., Real, M. I., Burrel, M., Forner, A., Sala, M., Brunet, M., ... Bruix, J. (2007). Chemoembolization of hepatocellular carcinoma with drug eluting beads: Efficacy and doxorubicin pharmacokinetics. *Journal of Hepatology*, 46(3), 474–481.
- Verret, V., Ghegediban, S. H., Wassef, M., Pelage, J. P., Golzarian, J., & Laurent, A. (2011). The arterial distribution of Embozene and Embosphere microspheres in sheep kidney and uterus embolization models. *Journal of Vascular and Interventional Radiology*, 22(2), 220–228.
- Weng, L., Rusten, M., Talaie, R., Hairani, M., Rosener, N. K., & Golzarian, J. (2013). Calibrated Bioresorbable microspheres: A preliminary study on the level of occlusion and arterial distribution in a rabbit kidney model. *Journal of Vascular and Interventional Radiology*, 24(10), 1567–1575.

SUPPORTING INFORMATION

Additional supporting information may be found online in the Supporting Information section at the end of this article.

How to cite this article: Lewis AL, Caine M, Garcia P, et al. Handling and performance characteristics of a new small caliber radiopaque embolic microsphere. *J Biomed Mater Res*. 2020;108B:2878–2888. <https://doi.org/10.1002/jbm.b.34619>